Human myotube formation is determined by MyoD-Myomixer/Myomaker axis

Haifeng Zhang, Junfei Wen, Anne Bigot, Jiacheng Chen, Renjie Shang, Vincent Mouly, Pengpeng Bi

DEVELOPMENTAL BIOLOGY

Human myotube formation is determined by MyoD–Myomixer/Myomaker axis

Haifeng Zhang[1], Junfei Wen[1], Anne Bigot[2], Jiacheng Chen[1], Renjie Shang[1,3],
Vincent Mouly[2], Pengpeng Bi[1,3]*

Myoblast fusion is essential for formations of myofibers, the basic cellular and functional units of skeletal muscles. Recent genetic studies in mice identified two long-sought membrane proteins, Myomaker and Myomixer, which cooperatively drive myoblast fusion. It is unknown whether and how human muscles, with myofibers of tremendously larger size, use this mechanism to achieve multinucleations. Here, we report an interesting fusion model of human myoblasts where Myomaker is sufficient to induce low-grade fusion, while Myomixer boosts its efficiency to generate giant myotubes. By CRISPR mutagenesis and biochemical assays, we identified MyoD as the key molecular switch of fusion that is required and sufficient to initiate Myomixer and Myomaker expression. Mechanistically, we defined the E-box motifs on promoters of Myomixer and Myomaker by which MyoD induces their expression for multinucleations of human muscle cells. Together, our study uncovered the key molecular apparatus and the transcriptional control mechanism underlying human myoblast fusion.

INTRODUCTION

Skeletal muscles account for around 40% of adult human body weight. The essential step of myogenesis that gives rise to the dimension of muscle tissues is myoblast fusion. During muscle development, many thousands mononucleated myoblasts recognize each other and fuse to form the elongated form of syncytium known as myofiber, the basic contractile unit of muscle tissues (1, 2). Similarly, regeneration of injured muscles also requires fusion of muscle stem cells with damaged myofibers (3–6). Myoblast fusion shares similarities with the fusion models of other cell types that generally involve cell recognition and adhesion, cytoskeletal reorganization, and, finally, membrane merging (5, 7–10). While major progresses were made that advanced our understanding of these processes, little was known about the molecular mechanism that is deployed at the membrane interface of myoblasts, which ensures the cell type specificity of fusion and also directs coalescence of plasma membranes.

Recent studies using murine models found two muscle-specific membrane proteins, Myomaker (*MymK*) and Myomixer (*MymX*, also known as Myomerger or Minion) (11–14). Specifically, deletion of MymK or MymX in mice abrogated the multinucleations of skeletal muscle tissues during embryo development. The loss of MymK or MymX in muscle stem cells also abolished myofiber regeneration in mice (15–17). Recessive mutations in MymK gene were also linked to a congenital myopathy with marked facial weakness (18, 19). Coexpression of MymX and MymK is sufficient to induce fusions between otherwise nonfusogenic cells, e.g., fibroblasts (12–14). Reconstitution experiments established a molecular model that shows that the fusion between two cells required the function of MymK on two sides, but that of MymX at least on one side (13). Therefore, MymX and MymK constitute the long-sought tissue-specific mechanism that drives multinucleations of skeletal muscles.

During mouse myogenesis, MymX and MymK share similar expression patterns with two members of myogenic regulatory factors

(MRFs), MyoD and MyoG (11–15). MyoD and the two MRF members, Myf5 and Myf6, are determinants of myogenesis (20–22). These myogenic factors display functional redundancy and reciprocal regulations of expression (20–24). Deletion of MyoD in mice led to genetic compensation from Myf5 and an overly normal myogenic program in vivo (25, 26). In adult mice, deletion of MyoD from satellite cells delayed regeneration, whereas deletions of both MyoD and Myf5 led to a complete failure of muscle regeneration (27). Consistent with the in vivo phenotype, mouse MyoD-deficient myoblasts showed defects of differentiation and fusion, although smaller myotubes can still be found in the culture (27). Compared with other MRFs, MyoG plays a major role at the later stage of myogenesis (28–30). Specifically, deletion of MyoG in vivo led to the near-complete absence of myofibers, whereas the isolated myoblasts from MyoG null mice retained normal myogenic potentials in culture (31). In zebrafish, deletion of MyoG down-regulated the expression of MymX and MymK genes (32), which are required for myoblast fusion that generates fast-twitch muscle fibers (18, 32–35).

Much of our knowledge about human myogenesis were gained from genetic studies using lower vertebrate model organisms. However, the unique molecular mechanism that dictates the tremendous size of human muscle cells is largely unknown. Here, we report the functions and regulations of MymX and MymK genes in the process of human syncytial myofiber formations. Using multiple lines of gene knockouts (KOs), we uncovered a molecular model whereby MymK is sufficient to drive human myoblast fusion, whereas MymX boosts fusion efficiency to generate heavily multinucleated myotubes. We also probed the functions of MRF family members during human myotube inductions. As the key molecular mechanism that governs this process, we show that MyoD is essential to control the formations of human myotubes. Specifically, genetic deletion of MyoD in human cells completely abolished myoblast differentiation and fusion. Although the differentiation potentials of human MyoD KO myoblasts can be efficiently rescued by Myf5 and Myf6, these factors showed much weaker effects on myoblast fusion. Using the approach of CRISPR-mediated interference, we revealed the *cis*-regulatory elements that MyoD uses to induce the transcription of human MymX and MymK genes. Together, our study provides insights into the molecular mechanism of human myoblast fusion.

[1]Center for Molecular Medicine, University of Georgia, Athens, GA 30602, USA.
[2]Center for Research in Myology UMRS974, Sorbonne Université, INSERM, Myology Institute AIM, Paris, France. [3]Department of Genetics, University of Georgia, Athens, GA 30602, USA.
*Corresponding author. Email: pbi@uga.edu

RESULTS

Drastic fusion defects upon genetic deletion of MymX in human myoblasts

The low-passage immortalized human myoblasts were derived from paravertebral muscle tissues of a healthy donor, as described previously (*36*). These cells display robust myogenic and fusogenic potentials. Shortly after 3 days of differentiation, majority of the cells formed huge syncytia that commonly contained hundreds of myonuclei (fig. S1A). This morphological change was accompanied by sharp inductions of the myogenic gene expression program, e.g., myosin heavy chain genes (MYH1, MYH3, and MYH8), MyoG, MYF6, and MEF2C (fig. S1B). The expression of other MRF members, MyoD and MYF5, was maintained at relatively high levels in the initial phase of differentiation but was down-regulated thereafter (fig. S1B).

In accordance with the timing of myoblast fusion, the expression of MymX and MymK was promptly and simultaneously induced by myogenic differentiation (fig. S1B). Although MymK expression can be stabilized during 3 days of differentiation, the abundance of MymX transcripts gradually diminished once it reached a plateau at 12 hours after myogenic induction. As a result, MymX protein peaked in a short time window but soon disappeared after 48 hours of differentiation (fig. S1C), which coincided with the near completion of fusion (fig. S1A). Western blotting analyses following cellular fractionations revealed the membrane localizations of MymX (fig. S1D) and MymK (fig. S1E) proteins in human myocytes. Therefore, the expression patterns of MymX and MymK in human cells closely mimicked those in murine muscles (*11–14*). However, the exact functions of MymX and MymK in human myoblasts are unknown.

We first performed loss-of-function study and generated human MymX KO (MymX^{KO}) myoblasts through CRISPR-Cas9–mediated gene editing (Fig. 1A). Briefly, a pair of guide RNA (gRNA) that targets MymX open reading frame (ORF) was delivered by lentiviral infection (Fig. 1B). Cells that express Cas9, but not gRNA, were deemed as wild-type (WT) control groups. MymX^{KO} clones were derived by single-cell isolations and clonal expansions. Genotyping analysis by sequencing revealed the editing and biallelic frameshift mutations of MymX gene (Fig. 1, C and D). Depletions of MymX protein were also confirmed by Western blotting analyses (Fig. 1E). Although the expression of myosin varied among MymX^{KO} clones at an early stage of differentiation, their levels were comparable with those from

Fig. 1. Loss of Myomixer causes major fusion defects of human myoblasts. (**A**) Schematic of CRISPR approach to generate gene KO single clone from human myoblasts. (**B**) Human MymX gene structure and positions of gRNAs and genotyping primers. (**C**) MymX genotyping results in three clones. Arrow points to the position of WT-size amplicon. (**D**) Sanger sequencing results of MymX genotyping polymerase chain reaction (PCR) products shown in (C). Biallelic deletions of MymX gene were confirmed. The frameshifted codons were highlighted in red. Arrow indicates the position of big deletion. (**E**) Western blots of myosin heavy chain (MF20) and MymX in human myoblasts after 40 or 72 hours of differentiation. DM, differentiation medium. (**F**) Myosin immunostaining results of WT and MymX^{KO} myoblasts. Cells were differentiated for 3 days. Arrow points to myotube. Scale bar, 100 μm. (**G**) Measurements of fusion of WT and MymX^{KO} myoblasts. *n* = 3. Statistical analysis was performed for the comparisons of multinucleated cells (three or more nuclei). ***$P < 0.001$. Data are means ± SEM. (**H**) Myosin immunostaining results to show the rescue of fusion defects of human MymX^{KO} myoblasts by retroviral MymX expression. Cells were differentiated for 3 days. Scale bar, 100 μm. (**I**) Confirmation of MymX reexpression by Western blotting.

WT cells after full-term differentiation (Fig. 1E). Consistently, MyoG, MYH8, and MymK were expressed at similar levels between genotypes (fig. S2A), indicating that the differentiation program of human muscle precursor cells was not affected by the absence of MymX protein.

Notably, deletion of MymX caused major fusion defects but did not eliminate all syncytium formations (Fig. 1F). In comparison with the massive myotubes that spread over large culture areas for the control group, 63% of MymX^{KO} cells remained mononucleated after full-term differentiation (Fig. 1G). The rest appeared as either binucleated myocytes or small myotubes that contained an average of 4.5 myonuclei (Fig. 1G). Similar results were recapitulated from another three MymX^{KO} clones (fig. S2, B to D). To verify that the fusion defect was attributed to the exact loss of MymX gene but not to a rare CRISPR off-target effect (if any), we performed rescue experiments. Fusion defects of MymX^{KO} cells can be faithfully rescued by introducing MymX expression construct that harbors silent mutations in the protospacer sequences of gRNAs (Fig. 1, H and I). Together, these results revealed the crucial role of MymX for human myotube formations.

Loss of MymK abolishes human myoblast fusion

Compared with mouse MymX^{KO} myoblasts that only rarely fused to generate small myotubes (*12–14*), large syncytia that host 6 to 10 myonuclei can be found in human MymX^{KO} culture (Fig. 1G). Although inactivation of MymX gene did not affect MymK expression (fig. S2A), we tested whether a higher level of MymK could induce a stronger fusion of MymX^{KO} myoblasts. Overexpression of human MymK in MymX^{KO} myoblasts significantly increased the abundance of multinucleations from which even larger syncytia were formed (fig. S3). This result indicated that human MymX^{KO} myoblasts can fuse in a MymK dosage-dependent manner. In comparison with mouse studies, these results indicate that the function of human MymK gene may be strengthened, which can replace the partial role of MymX. Alternatively, human myoblasts may use other muscle-specific factor(s) to assist the action of MymK in the absence of MymX.

To discern these possibilities, we first examined the role of MymK in human myoblasts by CRISPR mutagenesis (Fig. 2A). Genotyping and sequencing revealed biallelic frameshift mutations in all single clones (Fig. 2, B and C) except one allele in clone #G7 that showed in-frame deletions of 30 amino acids (Fig. 2C). Again, the loss of MymK did not affect myogenic differentiation, as normal expression levels for myosin and MyoG were detected (Fig. 2D and fig. S4A). Human MymK^{KO} myoblasts showed a complete failure of fusion because no muscle syncytium (three or more nuclei) was found after the full-term differentiation (Fig. 2, E and F). Same phenotypes were recapitulated from another three MymK^{KO} clones (fig. S4, B to D). Validating the specificity of CRISPR targeting, fusion defects of these human MymK^{KO} cells were rescued by introducing a gRNA-insensitive expression cassette for human MymK (Fig. 2G). Together, MymK is absolutely required for human myoblast fusion.

Human and mouse species share 80% homology for MymX proteins and 89% homology for MymK proteins. To strictly compare the fusogenic activities of these orthologs as a means to understand the mechanistic basis of human myoblast fusion, we generated human MymX and MymK double-KO (dKO) myoblasts by inactivating MymK gene in MymX^{KO} clone #G6 (fig. S5A). As expected, these cells can normally differentiate but do not fuse. The monoclonal antibody developed using mouse MymK antigen cannot faithfully recognize human MymK protein for us to gauge MymK overexpression levels (fig. S5B), a prerequisite of gene function assays. We opted to perform tagging for both human and mouse MymK proteins. Instead of using the conventional flag tag that disrupted MymK function (fig. S5C), we fused a diminutive EPEA (glutamic acid-proline-glutamic acid-alanine)–epitope tag, known as C-tag, to the C terminus of MymK (in short, MymK-C). Without losing MymK function (fig. S5C), this tagging method enabled us to unbiasedly measure the expression levels of human and mouse MymK proteins using a commercially available antibody that recognizes the EPEA sequence.

Consistently, reexpression of MymK-C in dKO cells rendered the low fusogenic activity that led to formations of small syncytia, which recapitulated the observations made from human MymX^{KO} culture (fig. S6A). Delivery of MymK-C together with MymX restored the normal-level fusion of dKO cells (fig. S6A). In these rescue assays, human and mouse MymX proteins did not show apparently different strength of fusogenic activity when their expression levels were also considered (fig. S6, A to C). However, the human MymK expression group displayed similar levels of rescue on fusion compared with those achieved by mouse MymK, although the protein abundance of human MymK was only one-third of that of mouse MymK (fig. S6, A to C). This indicates that human MymK may have higher fusogenic activity than mouse MymK. When similar expression level was achieved (fig. S6D), human MymK induced the formations of significantly larger syncytia than those from the mouse MymK expression group (fig. S6, E and F).

In addition to these rescue assays, we also examined human MymK function in a more stringent test involving nonmuscle cells. Expression of human MymK, in the absence of MymX, was not sufficient to induce fibroblast-fibroblast fusion (fig. 6, G and H), similar with previous observations of mouse MymK (*11*). Together, our results indicate that although human MymK displayed higher activities than mouse MymK, these proteins are not fundamentally different.

MymX promotes human myoblast fusion in the presence of MymK

The fusion defects of MymX^{KO} and MymK^{KO} cells highlight the critical requirements of these genes for optimal human myotube formations. We continued to probe the exact working model of MymX and MymK that drives syncytializations of human myoblasts. To distinguish fusion from cytokinesis defects, we performed dual-label and mixing experiments for three genotypes of human myoblasts: WT, MymX^{KO}, and MymK^{KO} (Fig. 3A). This allows the tracking of cell fusion because the merging of cells from two different groups (termed as heterologous fusion) can be reported by mixing of fluorescence signals.

These fusion-reconstitution experiments showed that MymK^{KO} myoblasts cannot fuse with themselves, nor with MymX^{KO} or WT myoblasts (Fig. 3, B and C), indicating that MymK is required from both sides for membrane coalescences. Consistent with our earlier observations, MymX^{KO} myoblasts can fuse to generate syncytia that host an average of four myonuclei (Fig. 3, B and C); however, when MymX is present on one side, as modeled by the WT and MymX^{KO} cell mixing, larger syncytia that contained an average of 57 myonuclei were formed (Fig. 3, B and C); furthermore, when MymX was present on both sides, as modeled in WT-WT mixing scheme, an average of 354 myonuclei per syncytium was scored (Fig. 3, B and C). Together, these results revealed an interesting molecular model of
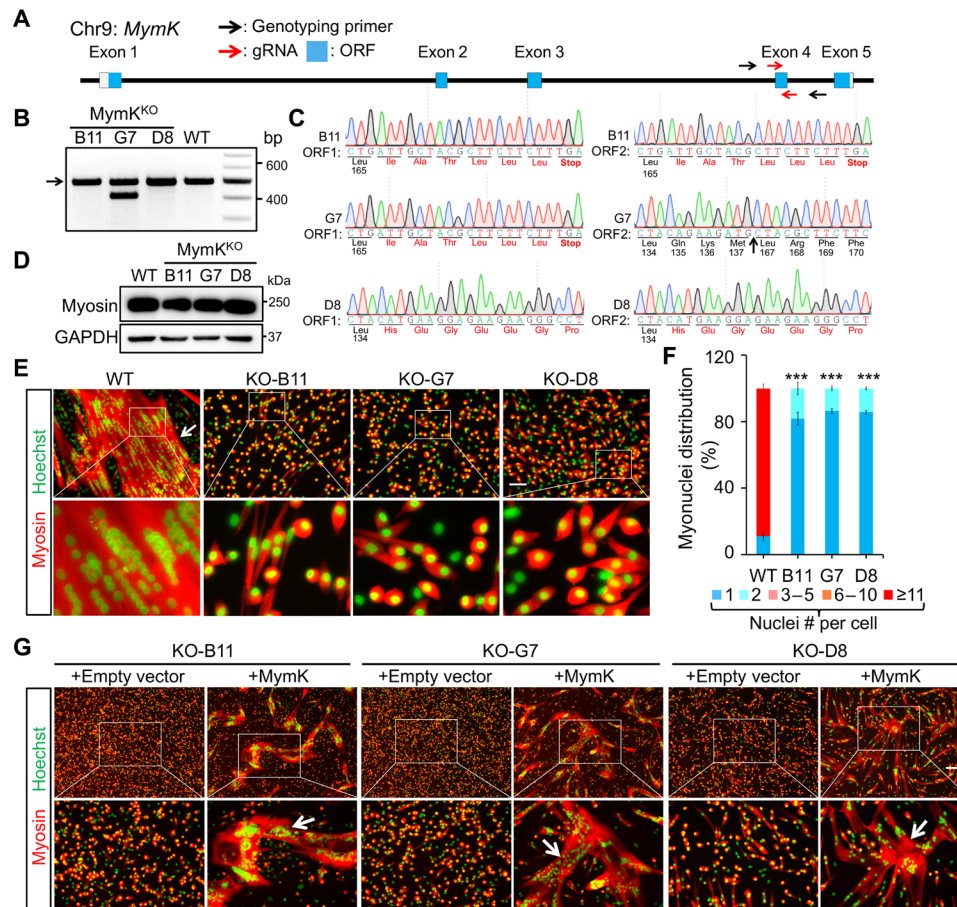
Fig. 2. Complete loss of syncytial myotubes upon deletion of MymK gene in human myoblasts. (**A**) Human Myomaker (MymK) gene structure and the positions of gRNAs and genotyping primers. (**B**) MymK genotyping results for three KO clones. Arrow points to the position of WT-size amplicon. (**C**) Sanger sequencing results of MymK genotyping PCR products as shown in (B). The frameshifted codons were highlighted in red. Arrow indicates the position of big deletion. (**D**) Western blot analysis of myosin heavy chain. Cells are differentiated for 3 days. (**E**) Myosin immunostaining results of WT and MymK^{KO} myoblasts. Cells were differentiated for 3 days. Arrow points to multinucleated myotube. Nuclei were counterstained with Hoechst and pseudo-colored in green. Scale bar, 100 μm. (**F**) Measurements of fusion for myosin$^+$ WT and MymK^{KO} myoblasts. $n = 3$. The ratio of mononuclear cells was used for statistical analysis. ***$P < 0.001$. Data are means ± SEM. (**G**) Myosin immunostaining results to show the rescue of fusion defects of human MymK^{KO} myoblasts by retroviral MymK expression. Cells were differentiated for 3 days. Scale bar, 100 μm.

human myoblast fusion that MymK on both sides can induce low-grade fusions independent of MymX, whereas the presence of MymX on one or two sides markedly boosts the fusion efficiency. Consistently, we show that, even in the absence of myogenic cues (missing MymX expression), syncytia from WT myoblasts can be induced when MymK was ectopically expressed; larger syncytia were formed when MymX protein was also provided (Fig. 3D). Together, these results highlight the functional synergy between MymX and MymK that is required for optimal fusion of human myoblasts.

MyoD is essential for MymX/MymK expression and human myoblast fusion

Myoblast fusion is a tightly regulated process that ensures the cell type specificity and also avoids any undesirable fusion of muscle cells. This could be achieved by controlling the expression of MymX and MymK specifically in muscle cells and precisely in the time window of myoblast fusion. As such, the transcriptional mechanism that determines the spatial and temporal expression patterns of MymX and MymK genes is critical for proper progression of myogenesis.

Previous analyses of MymX and MymK promoters indicated that MyoD may control MymX and MymK expression in mouse myoblasts (11, 12, 15). However, a direct test of these regulations by KO experiments is missing. Contrary to the perinatal lethality phenotype of MymX or MymK mutants, MyoD null mice appeared normal and fertile and did not show any overt muscle phenotypes (25, 26). In adult mice, MyoD null myoblasts also partially retained fusogenic capacity that can support skeletal muscle regeneration (27), although the loss of either MymX or MymK abolished muscle regeneration (15, 16).

Beyond the apparent phenotypic differences among those murine models of gene KOs, the effects of MyoD deletion in human cells also remain untested. To directly examine the regulatory roles of MyoD on MymX and MymK expression, we generated human MyoD^{KO} myoblasts by CRISPR mutagenesis with a gRNA that targets the first coding exon of MyoD gene. Sequencing analysis of genotyping polymerase chain reaction (PCR) products revealed biallelic disruptions of MyoD ORFs in two clones (Fig. 4A and fig. S7, A and B). Depletions of MyoD protein in human MyoD^{KO} myoblasts were confirmed by immunostaining (Fig. 4B, top row). Notably, the
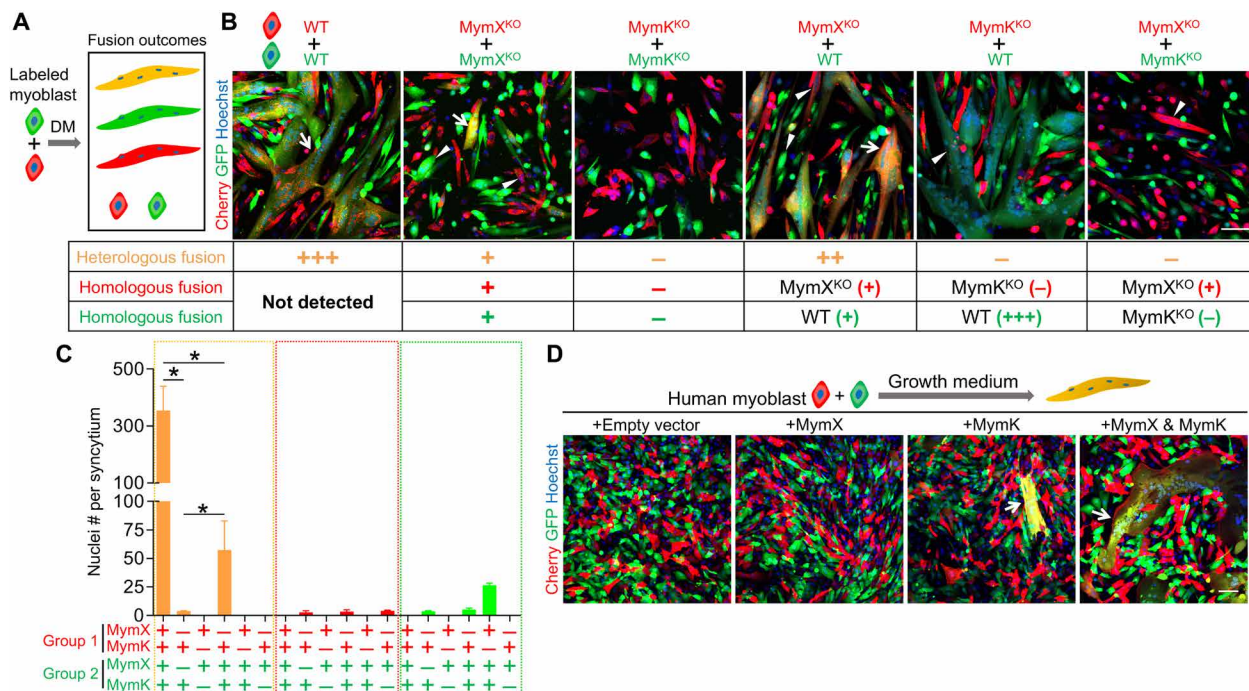
Fig. 3. MymX promotes human myoblast fusion in the presence of MymK. (**A**) Schematic of fusion reconstitution assays. Human myoblasts were first labeled by the expression of green fluorescent protein (GFP) or red fluorescent protein Cherry. Equal numbers of labeled myoblasts were then mixed and differentiated for 3 days. (**B**) Representative fluorescence images that distinguish homologous fusion (Cherry$^+$ or GFP$^+$) from heterologous fusion (Cherry$^+$/GFP$^+$) for six mixing combinations from three genotypes (WT, MymX^{KO}, and MymK^{KO}). Arrows point to the heterologous syncytia; arrowheads point to the homologous syncytia. MymX^{KO} clone #G6 and MymK^{KO} clone #G7 were used for mixing experiments. Scale bar, 100 μm. Fusion outcomes were scored: −, no fusion; +, basal level fusion; ++, intermedium level fusion; +++, high level fusion. (**C**) Quantification results of fusion for experiments as performed in (B). $n = 3$. *$P < 0.05$. Data are means ± SEM. (**D**) Retroviral expression of human MymK in WT human myoblasts in growth condition is sufficient to induce syncytium formation. Fusion was boosted when human MymX was coexpressed together with MymK. Arrows point to multinucleated cells with dual labels. Scale bar, 100 μm.

loss of MyoD abolished the fusion and differentiation of human myoblasts evidenced by the complete absence of myosin expression and syncytium formation after full-term myogenic inductions (Fig. 4B, second row). Accordingly, the expression of MyoG, MymX, and MymK was also lost in MyoD^{KO} cells (Fig. 4, C and D). These myogenic and fusogenic defects were rescued when exogenous MyoD was provided (Fig. 4, E and F). Therefore, human myoblasts fully depend on MyoD for myotube formations in culture.

MyoG is a downstream target gene of MyoD during myoblast differentiation (*31*, *37*). Expression of MyoG was abolished in human MyoD^{KO} myocytes (Fig. 4, C and D). When MyoG was ectopically provided in MyoD^{KO} cells, the expression of MymX and MymK genes (Fig. 4, G and H) as well as myotube formations (Fig. 4, I and J) were restored to comparable levels as achieved by MyoD rescue. These results indicate that MyoD may control human myotube formations through MyoG.

MyoG promotes human myoblast fusion by increasing MymK expression

To directly examine the role of MyoG downstream of MyoD during human myogenesis in vitro, we knocked out MyoG gene through CRISPR-Cas9–mediated gene targeting. Genotyping and sequencing analyses revealed homozygous deletions of 164 base pairs (bp) within the first exon of MyoG in two clones (Fig. 5A and fig. S8, A and B). As a consequence, a premature stop codon emerged in this exon. The truncated myogenin transcripts from MyoG^{KO} cells were expressed

at a level similar to that of the full-length myogenin transcripts from WT cells, as detected by reverse transcription PCR (Fig. 5B) and quantitative PCR (qPCR) (Fig. 5, C and D), indicating the insensitivity of this mutated transcript to nonsense-mediated mRNA decay. Nevertheless, the absence of myogenin protein in MyoG^{KO} clones was confirmed by Western blotting (Fig. 5E) and immunostaining (Fig. 5F) analyses using an antibody that detects the C terminus of MyoG protein.

Unexpectedly, in contrast to the complete loss of muscle cells in human MyoD^{KO} culture, MyoG^{KO} cells displayed relatively moderate phenotypes, i.e., 52% reductions of the differentiation index (Fig. 5, F and G) and 65% reductions of the fusion index (Fig. 5, F and H), compared with the control group. However, reflecting the combined effects, MyoG^{KO} culture showed much smaller syncytia that contained an average of 12 myonuclei, compared with 119 myonuclei per syncytium scored in the control group (Fig. 5I). The fusion defect is accompanied by a 62% reduction of MymK mRNA level in MyoG^{KO} myoblasts (Fig. 5C). By comparison, the expression of MymX at both mRNA (Fig. 5C) and protein (Fig. 5E) levels was not significantly affected by the deletion of MyoG. To consolidate this and the role of MyoG in human myoblast differentiation, we also checked the expression of MymX and myosin by Western blotting analyses at more time points along the course of myogenic differentiation. Consistently, MyoG^{KO} myoblasts expressed normal levels of MymX, although the expression of myosin was slightly delayed at early stages of differentiation (Fig. 5J and fig. S8C).
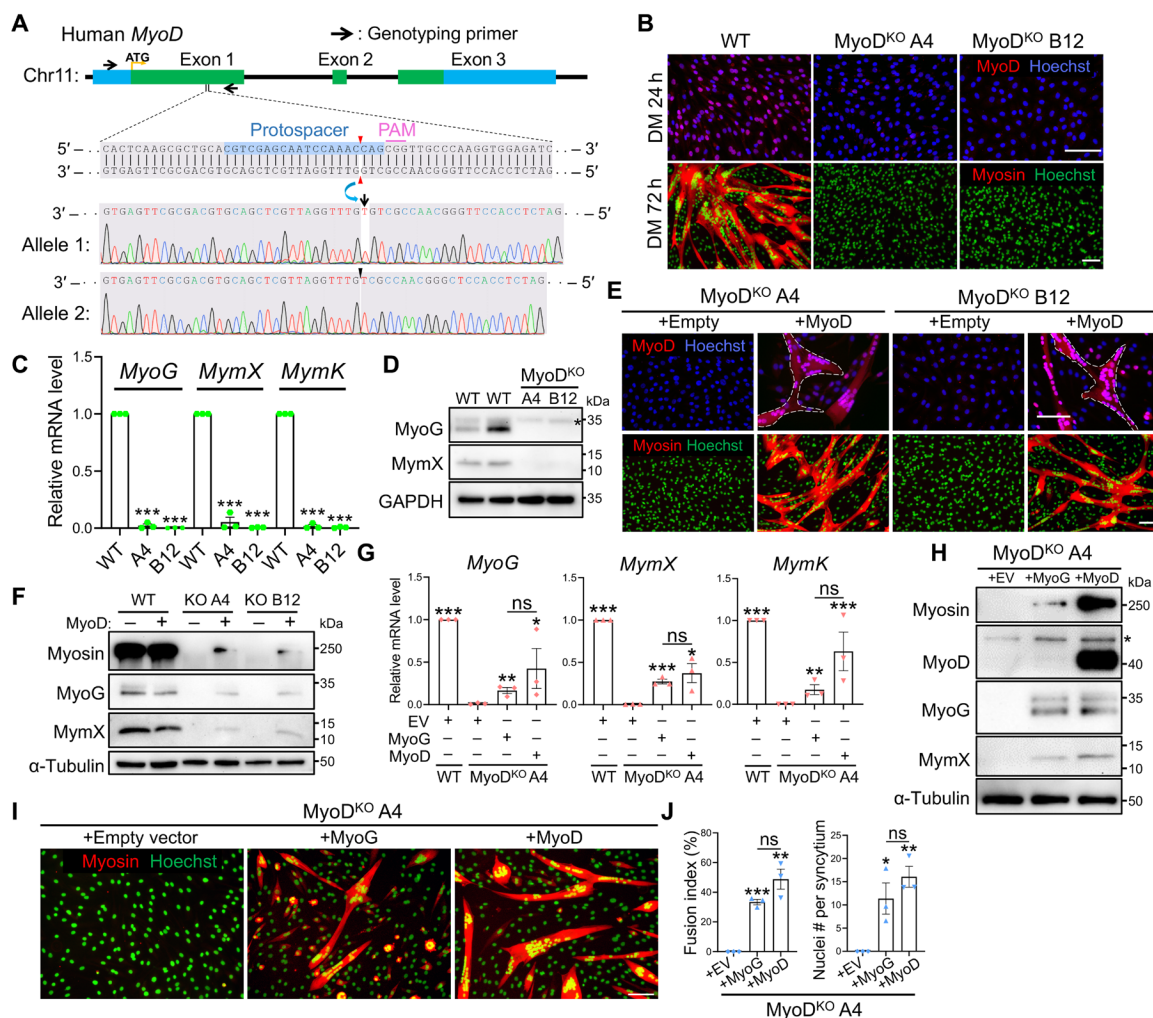
Fig. 4. Deletion of MyoD abolishes human myotube formation. (**A**) MyoD gene structure and Sanger sequencing results that confirmed biallelic frameshift mutations of MyoD in human myoblasts (clone #A4). Arrow points to an insertion; arrowhead points to a deletion. (**B**) Immunostaining results of human WT and MyoD^{KO} myoblasts. MyoD staining confirmed depletions of MyoD protein in MyoD^{KO} myoblasts. Myosin staining showed the absence of differentiation and fusion in the MyoD^{KO} group. Scale bar, 100 μm. (**C**) Quantitative PCR (qPCR) results of myoblasts differentiated for 48 hours. (**D**) Western blots of myogenin and MymX in human MyoD^{KO} myoblasts (DM 1 day). Star indicates a nonspecific band. (**E**) Immunostaining results of MyoD (top) and myosin (bottom) to show rescue of myogenic defects for MyoD^{KO} myoblasts by retroviral expression of MyoD (DM 3 days). Scale bar, 100 μm. (**F**) Western blot analyses of myosin, myogenin, and MymX in WT and human MyoD^{KO} myoblasts with or without retroviral expression of MyoD (DM 2 days). (**G**) qPCR results of WT and MyoD^{KO} myoblasts with the expression of MyoG or MyoD (DM 2 days). (**H**) Western blot to show the expression of myosin, MyoD, MyoG, and MymX in MyoD^{KO} myoblasts with retroviral expression of MyoG or MyoD (DM 1.5 days). (**I**) Myosin immunostaining results of human MyoD^{KO} myoblasts with retroviral expression of MyoG or MyoD (DM 3 days). Scale bar, 100 μm. (**J**) Quantification results for experiments shown in (I). $n = 3$. ns, not significant; *$P < 0.05$; **$P < 0.01$; ***$P < 0.001$. Data are means ± SEM.

To understand the mechanism underlying MyoG^{KO} phenotype, we performed rescue experiments. Consistent with a role of MymK, overexpression of this gene markedly increased the sizes of MyoG^{KO} myotubes (Fig. 5, K and L). Similar rescue effects from MymK were also observed in another MyoG^{KO} clone (fig. S8, D and E). Immunostaining revealed that MyoG^{KO} cells normally expressed MyoD at 1 day after myogenic inductions (fig. S9A). Considering that the expression level of MyoD declines after this stage (fig. S1B), we tested whether an extended presence of MyoD protein in MyoG^{KO} cells could alleviate their fusogenic defects. Overexpression of MyoD in MyoG^{KO} cells restored the fusion and differentiation indexes to comparable levels as achieved by reexpression of MyoG itself (fig.

S9, B to D). Accordingly, MymK expression in MyoG^{KO} cells was also normalized by the ectopic expression of MyoD (fig. S9E). The reciprocal rescues of the myogenic defects among these KO cells by MyoD or MyoG highlight an interesting paradigm of human myotube formation that, at the early stage of myogenesis, MyoD initiates the myogenic program and MyoG expression; toward the later stage when MyoD expression declines, MyoG can work as a surrogate of MyoD to continually sustain muscle fusion that boosts the sizes of human myotubes by maintaining MymK transcription. This model is consistent with murine data that the regulations of a myogenic program by MyoD and MyoG do not overlap with each other (*31*).
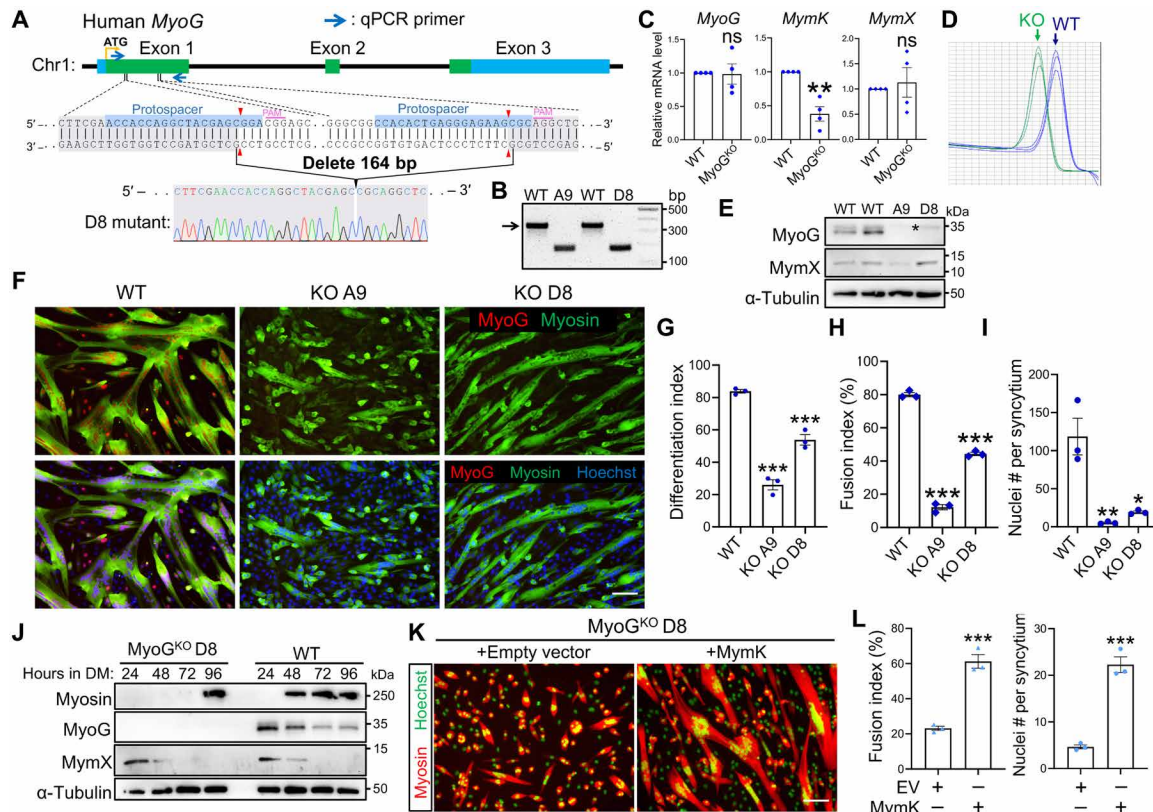
Fig. 5. MyoG boosts MymK expression and human myoblast fusion. (**A**) MyoG gene structure and Sanger sequencing results that confirmed biallelic deletions of MyoG. (**B**) Reverse transcription PCR results using primers shown in (A). Arrow points to the position of WT-size (341 bp) amplicon. KO band is 177 bp. (**C**) qPCR results of human WT and MyoG^KO myoblasts. $n = 4$. (**D**) Melting curve plots of MyoG qPCR amplicons generated from WT and MyoG^KO cDNA samples shown in (C). (**E**) Western blots of myogenin and MymX in human WT and MyoG^KO myoblasts (DM 1.5 days). Star indicates a nonspecific band. (**F**) Myosin and myogenin immunostaining results of human WT and MyoG^KO myoblasts. MyoG staining confirmed the depletion of MyoG proteins in MyoG^KO clones. Myosin staining revealed relatively normal myoblast differentiation and moderately decreased fusion when MyoG was deleted (DM 2 days). Scale bar, 100 μm. (**G** to **I**) Measurements of differentiation index (G), fusion index (H), and averaged nuclei number per syncytium (I). (**J**) Western blots of myosin, MyoG, and MymX at various stages of myoblast differentiation. (**K**) Myosin immunostaining results to show the rescue of fusion defects of human MyoG^KO myoblast (clone #D8) by retroviral expression of MymK (DM 3 days). Scale bar, 100 μm. (**L**) Quantification results of fusion for the experiments shown in (K). $n = 3$. ns, no significant difference. $*P < 0.05$, $**P < 0.01$, $***P < 0.001$. Data are means ± SEM.

MYF5 and MYF6 cannot fully substitute functions of MyoD for human myoblast fusion

Genetic studies revealed the loss of most myogenesis and perinatal lethality when MyoG was inactivated in mice (*28–31*). Mice lacking either MyoD or Myf5 showed normal myogenesis, whereas mice lacking both factors failed to generate muscle cells (*25, 31, 38–40*). The phenotypic disparities among these null alleles of these factors highlight the functional redundancy of MRF members and different compensation responses in these systems. We continued to dissect the roles of other MRF members in human MyoD^KO myoblasts. First, we examined the expression of MYF5, MYF6, and MEF2C, another myogenic factor that plays important roles during the late-stage myogenesis (*41, 42*). Compared with WT cells, human MyoD^KO myoblasts showed normal and decent levels of expression of MYF5 but great reductions for the expression of MYF6 and MEF2C (fig. S10A).

We then tested whether overexpression of MYF5 or the normalized expression of MYF6 and MEF2C could restore the myogenic potentials of human MyoD^KO myoblasts. Exogeneous expression of any of these factors robustly rescued myogenic differentiation, i.e., restorations of around 30% differentiation index (fig. S10, B to D). In contrast, only MYF5 and MYF6 can weakly induce the fusion and

generations of small myotubes that hosted three to four nuclei on average (fig. S10, C and E). These fusion-rescue effects corelated well with the induction levels for the expression of MymX and MymK genes (fig. S10F). Consistent with stronger effects on differentiation, all three myogenic factors strongly induced myosin expression (fig. S10F). Together, the functions of MyoD during human myotube formations in vitro cannot be replaced by other MRF members.

MyoD is self-sufficient to induce the transcription of MymX and MymK

The above gain- and loss-of-function assays highlight the essential roles of the MyoD–MymX/MymK axis in controlling human myoblast fusion. However, the mechanistic details underlying the gene regulations remained unclear. For instance, is MyoD self-sufficient to initiate MymX and MymK expression independent of other myogenic factors? If yes, how does MyoD transactivate MymX and MymK expression?

We investigated the first question by performing sufficiency tests in fibroblasts that do not have the expression of myogenic factors. We show that transduction of MyoD into 10T1/2 fibroblasts robustly induced MymX and MymK expression (Fig. 6A) as well as the
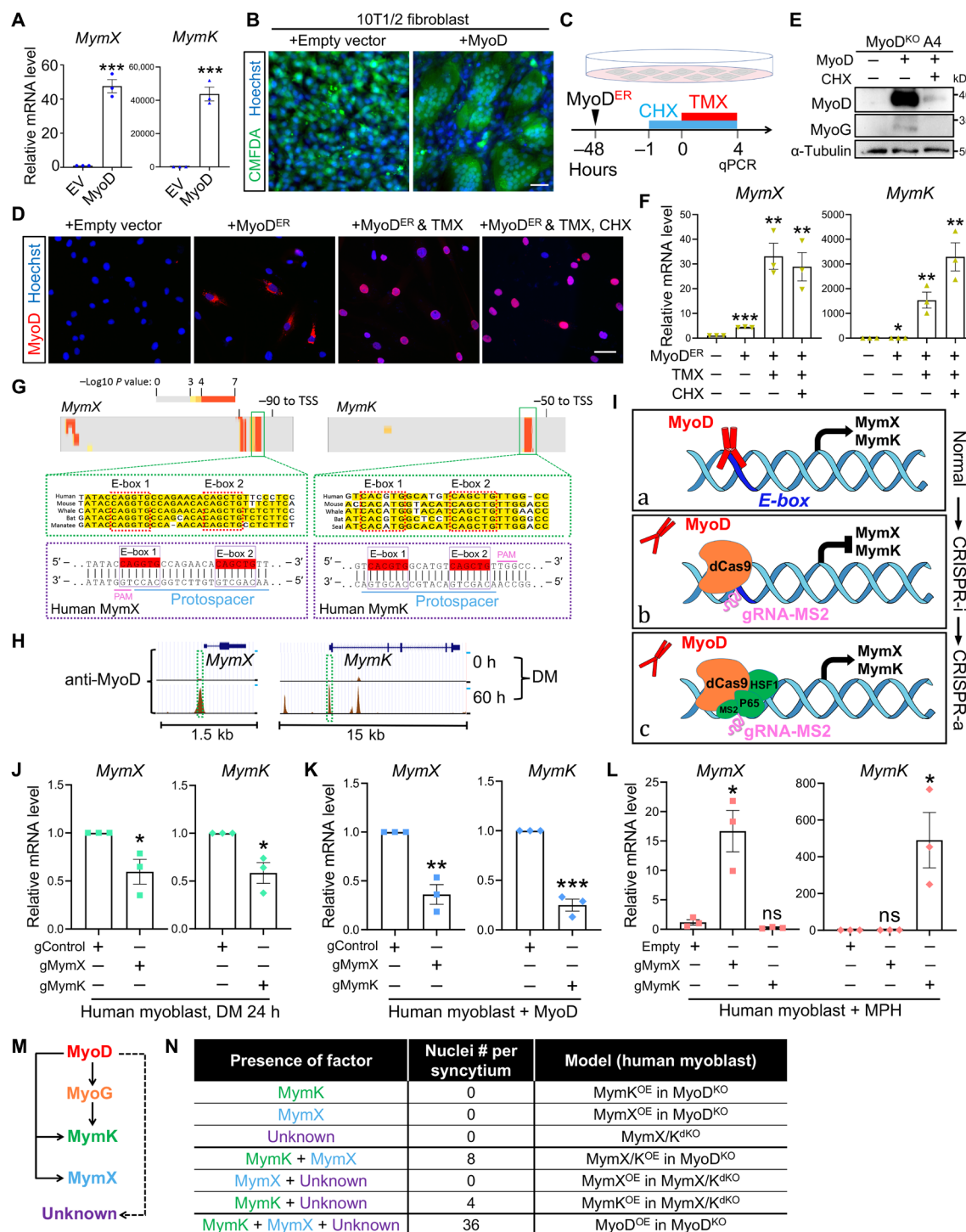
Fig. 6. MyoD is self-sufficient to induce MymX and MymK transcription. (**A**) qPCR results of 10T1/2 fibroblasts. (**B**) Fluorescence images of cell cytosol dye CMFDA (5-chloromethylfluorescein diacetate) to highlight syncytialization induced by MyoD. Scale bar, 100 μm. (**C**) Schematic of experiment design. (**D**) MyoD immunostaining results. Scale bar, 50 μm. (**E**) Western blot of MyoD[KO] myoblasts in conditions specified. Note that MyoG expression was blocked by CHX (treated 24 hours). (**F**) qPCR results of fibroblasts after treatments shown in (C). (**G**) Predictions of MyoD motifs on promoters of MymX (left) and MymK (right) from distantly related mammalian species. Proto-spacer sequences of gRNAs that were used in CRISPR experiments (I to L) were provided. TSS, transcriptional start site. (**H**) ENCODE ChIP-seq results of MyoD from mouse myoblasts. Green box highlights the mouse sequence in (G). (**I**) Experiment design to probe *cis*-regulatory elements by dCas9-mediated interference. CRISPRi, CRIPSR inhibition; CRISPRa, CRISPR activation. MS2 loop on gRNA can bind with transactivator MPH (MS2-P65-HSF1). (**J** to **L**) qPCR results of human WT myoblasts in conditions specified. gControl is gRNA that binds to an upstream non–E-box region on the promoter of human MymX or MymK. n = 3. *P < 0.05, **P < 0.01, ***P < 0.001. Data are means ± SEM. (**M**) Summary of gene regulations during human myoblast fusion. Dot line indicates regulation of the unknown factor(s) by MyoD. This yet-to-be-defined factor is essential for MymK function especially in the absence of MymX. (**N**) Comparisons of gene function during myoblast fusion suggested by data in figs. S6 and S10.

fibroblast-syncytia formations (Fig. 6B). This myogenic fate conversion driven by MyoD involves global gene expression changes, including up-regulations of a panel of myogenic factors downstream of MyoD (43–46). To rule out the secondary effects of MyoD-responsive genes in regulations of MymX and MymK expression, we concomitantly inhibited protein translations by cycloheximide (CHX) with the control of MyoD transcriptional activities (Fig. 6C). The latter was achieved by commanding nuclear importing of a MyoD–estrogen receptor fusion protein (MyoD^{ER}) (47) with treatment of 4-hydroxytamoxifen (4OH-TMX). We reasoned that if MyoD is self-sufficient in activating MymX and MymK expression, such an induction will not be negated by CHX treatment, which blocks translations of other myogenic factors; by contrast, if CHX compromises the action of MyoD, it would suggest that MyoD also requires the function of other myogenic factors to initiate MymX and MymK expression.

We first validated our experimental design and reagents. Treating cells with 4OH-TMX promptly induced nuclear localization of MyoD^{ER} protein, as revealed by immunostaining of MyoD (Fig. 6D). Using MyoG as an example, we show that CHX can efficiently block protein synthesis in response to MyoD function (Fig. 6E). With these technical validations, we examined the impact of CHX on MyoD-induced MymX and MymK expression. Notably, MyoD^{ER} robustly induced transcriptions of MymX and MymK genes from fibroblasts in the absence and presence of CHX (Fig. 6F). Therefore, the transactivator MyoD, independent of other myogenic factors, is sufficient to commence MymX and MymK expression.

The sufficiency of MyoD in inducing MymX and MymK expression necessitates a clear understanding of the molecular mechanism underlying this process. As a basic helix-loop-helix transcriptional factor, MyoD activates the expression of its target genes by binding to E-box motifs (CANNTG) (45). Using FIMO, a motif discovery tool that empirically predicts transcriptional factor binding sites (48), we found two MyoD-binding motifs that were highly conserved in proximal promoters of MymX (Fig. 6G, left) and MymK (Fig. 6G, right) from five distantly related mammal species including whale and bat. Analysis of an ENCODE chromatin immunoprecipitation sequencing (ChIP-seq) dataset (49) revealed that in C2C12 myoblasts that underwent fusion, MyoD can bind to the predicted promoter regions that centered on the two highly conserved E-box motifs (Fig. 6H).

We then used a CRISPR tool to interrogate gene regulatory networks as previously reported (50–52). For this experiment, a catalytically dead Cas9 (dCas9) was applied to dissect the function of the E-box motifs underlying the MyoD–MymX/MymK axis (Fig. 6I). We hypothesized that MyoD can bind to certain E-box motifs to induce MymX and MymK expression during normal differentiation (Fig. 6I, state a); when recruited by gRNA, the positioning of dCas9 to the proximity of E-box motifs and the unwinding of the DNA should block MyoD binding, thus repressing the transcriptions of MymX and MymK genes (Fig. 6I, state b); as a proof of the gRNA targeting specificity, MymX and MymK expression should be rescued when the transactivator MPH (MS2-P65-HSF1) is provided and recruited to MymX and MymK promoter regions by docking to an MS2 loop on these gRNAs (Fig. 6I, state c). Consistent with our hypothesis, the expression of gRNA that recruits dCas9 to the E-box on the MymX promoter significantly inhibited either differentiation-activated (Fig. 6J, left) or MyoD overexpression–induced (Fig. 6K, left) MymX expression in human myoblasts. Similar effects were also observed using a gRNA

that binds to the E-box region on the MymK promoter (Fig. 6, J, right, and K, right). In these assays, gRNA that targeted an upstream non–E-box region on MymX or MymK promoters was applied as control. Last, adding transactivator MPH successfully switched the MymX or MymK transcription state from inhibition to activation in a gRNA-specific manner (Fig. 6L). Together, these results indicate that MyoD directly activates MymX and MymK expression by binding to the evolutionarily conserved E-box motifs on MymX and MymK promoters, respectively.

In summary, our results provide the genetic evidence that human myoblast fusion is determined by the MyoD–MymX/MymK regulatory axis (Fig. 6M). One intriguing observation is that MymK can promote low-grade fusion of human MymX^{KO} myoblasts (fig. S3) but failed to induce fibroblast-fibroblast fusion (fig. S6, G and H). This result indicates that, in the absence of MymX, MymK requires additional muscle-specific factor(s) to activate the cell fusion program. Consistent with this notion, we show that the expression of MymK cannot induce fusion of human MyoD^{KO} myoblasts (fig. S10, G and H). Although coexpression of MymK together with MymX can induce fusion of MyoD^{KO} myoblasts, the efficiency was not as high as that elicited by MyoD reexpression (fig. S10, G and H). Therefore, this additional factor, similar to MymX and MymK, could also receive regulations from MyoD during human myoblast differentiation. On the basis of our gain/loss-of-function tests, functional comparisons of these factors and their combinations were highlighted (Fig. 6N). Together, our study revealed the key molecular mechanism that governs human myoblast fusion.

DISCUSSION
Using gene KO experiments, we uncovered the crucial function of MymX, MymK, and MRF regulators during human myoblast differentiation and fusion. With these unique gene KO reagents, we also carefully compared the fusogenic activities of human and mouse MymX/MymK orthologs. Contrary to a protein homology–assisted prediction, human MymK, instead of MymX, showed higher activities compared with their mouse orthologs. Even in the absence of MymX, MymK protein can induce low-level myoblast fusion in a dosage-dependent manner. Future endeavors are needed to study the biochemical basis underlying the functional gain of human MymK protein.

MymX and MymK expression ought to be tightly controlled for proper multinucleations of myoblasts in coordination with differentiation program. Our functional studies of MyoD, MyoG, and other MRFs highlight the distinct contributions of these factors in governing human myoblast fusion. Specifically, MyoD is essential and sufficient to transactivate the fusion program. Even in the absence of other myogenic factors, MyoD induced MymX/MymK expression and robust syncytializations. Despite being a direct target gene of MyoD, MyoG is not absolutely required for human myoblast fusion but can promote this process by increasing MymK expression. This result aligned well with a recent report that disruption of MyoG gene in zebrafish does not prevent myogenic differentiation but instead drastically compromised myocyte fusion and significantly reduced myotube sizes (32). MyoD and MyoG can form heterodimer that binds to E-box motifs and induces the expression of common target genes (45, 53). This may also be true for MymK transcription at the early stage of human myoblast differentiation. By contrast, MymX expression was not affected by the loss of MyoG. Consistent

with the notion that MyoG does not control MymX expression in human myoblasts, our characterizations of gene expression during human myoblast differentiation showed that the changes of MymX expression preceded the dynamics of MyoG expression (fig. S1B).

The selective boost of MymK expression by MyoG is intriguing, especially in the context that MyoG relays the role of MyoD toward the late stage of myoblast fusion (37). As a consequence, the time window of MymK expression and function may extend beyond that of MymX. In theory, this expression pattern can establish the cell identities of fusion: MymK$^+$ myofibers and MymK$^+$/MymX$^+$ myocytes. On the basis of our quantitative analyses of fusion efficiency controlled by side requirements of MymX (Fig. 3C), it predicts three fusion schemes: (i) Myocyte-myocyte fusion is most efficient because MymX is present on both sides; (ii) myocyte-myofiber fusion is less efficient because MymX is only present on one side (myocyte); and (iii) myofiber-myofiber fusion is least efficient because MymX is absent from both sides. This three-phase fusion model could orderly correspond to three-stage human myogenesis in culture (fig. S1A): formations of nascent myofibers at the early stage (day 1), myofiber growth through nuclear additions in the middle stage (day 2), and final adjustment of myofiber size versus number at the late stage (day 3). Consistent with this model, the phenotype of human MyoG^{KO} myoblasts may represent a state of arrested fusion that nascent myotubes were formed but failed to grow to normal sizes like the control group (Fig. 5F). In addition, we did observe the fusion between myoblasts and mature myotubes in cell label–mixing experiments, where MymX is only detected in the former, but not the latter, cell population (fig. S10, I to K).

It is well known that members of the MRF family often exhibit functional redundancies in vivo, but not in cultured cells (26, 29). For instance, the loss of MyoD in vivo can trigger an up-regulation of Myf5 expression that can efficiently compensate and support myogenesis (25, 27, 38). In comparison, myogenic defects in primary cultures of mouse MyoD^{KO} myoblasts were pronounced, although low-level fusions were still observed (27, 54–56). Our results showed that deletion of MyoD in human myoblasts did not affect the expression level of MYF5, yet it also failed to safeguard a myogenic program for MyoD^{KO} myoblasts. Although overexpression of MYF5 or MYF6 partially rescued the differentiation of human MyoD^{KO} cells, these genes only showed minor effects on MymX/MymK expression and myoblast fusion. A possible explanation is that even if MYF5 binds to the same promoter site, it displays weaker activities compared with MyoD (57). Our analysis of the *cis*-regulatory elements identified two conserved MyoD-binding E-box motifs on the promoters of human MymX and MymK genes. The competing binding of these motifs by the dCas9-gRNA complex significantly inhibited but failed to completely block the inductions of MymX and MymK expression in response to MyoD. This suggests that, in addition to these tested E-box motifs in the proximal promoters, MyoD may also use other distal E-box motifs to fine-tune MymX and MymK expression. Therefore, future efforts are needed to comprehensively study the potential function of other regulatory elements in controlling human myoblast fusion.

Last, the transcriptional mechanism by which MyoG uses to differentially induce MymK and MymX expression in human myoblasts remains unknown. This will need to be explained based on the distinct settings of MyoG loss- versus gain-of-function experiments. Specifically, although MymX expression was not changed upon deletion of MyoG, overexpression of MyoG can robustly induce the expression of both MymX and MymK in human MyoD^{KO} myoblasts. In zebrafish, MyoG was shown to bind to the MymK promoter to directly activate its expression (32). Analysis of the ENCODE ChIP-seq data (49) also revealed the co-occupancy of MyoG with MyoD on promoters of MymX and MymK in mouse myoblasts. Therefore, we predict that the evolutionarily conserved regulatory mechanism could also be deployed in human cells by which MyoG controls MymK expression at the late stage of myogenesis, whereas MymX expression is independent of a similar regulation mechanism by MyoG.

MATERIALS AND METHODS
Cell cultures
Human myoblasts (hSkMC-AB1190) were immortalized as we previously published (36). These cells were cultured in 15% fetal bovine serum (FBS) and 5% Growth Medium Supplement Mix in Skeletal Muscle Cell Basal Medium with 1× GlutaMAX and 1% gentamicin sulfate. Fibroblasts were maintained in 10% FBS with 1% penicillin-streptomycin in Dulbecco's modified Eagle's medium (DMEM). Myoblast differentiation medium contained 2% horse serum in DMEM with 1% penicillin-streptomycin. Cells do not have mycoplasma contamination as tested by using the Universal Mycoplasma Detection Kit (American Type Culture Collection, 30-1012K).

Lentivirus preparation and CRISPR-Cas9 KO experiments in cultured cells
The Lenti-CRISPR v2 vector (58) was a gift from F. Zhang (Addgene plasmid #52961). The following gRNAs that target the coding regions of human MymX, MymK, MyoD, and MyoG genes were individually cloned into the Lenti-CRISPR v2 vector: MymX gRNA 1 (5′→3′), GGCTCCCAGGACATGCGAG; MymX gRNA 2 (5′→3′), ACCTCTCCCTCCTCTCCAGG; MymK gRNA 1 (5′→3′), CTCACAGCTACAGAAGATGA; MymK gRNA 2 (5′→3′), AAAGAAGAAGCGTAGCATCA; MyoG gRNA 1 (5′→3′), ACCACCAGGCTACGAGCGGA; MyoG gRNA 2 (5′→3′), CCACACTGAGGGAGAAGCGC; MyoD gRNA (5′→3′), CGTCGAGCAATCCAAACCAG.

For lentivirus production, Lenti-X 293T cells (Clontech, 632180) were cultured in DMEM (containing 1% penicillin-streptomycin and 10% FBS). Transfection was performed using FuGENE6 (Promega, #E2692) with psPAX2 and pMD2.G plasmids. Two days after transfection, lentivirus supernatant was filtered and concentrated with the Lenti-X Concentrator (Clontech, PT4421-2) following the manufacturer's protocol. The psPAX2 vector was a gift from D. Trono (Addgene plasmid #12260). The pMD2.G vector was a gift from D. Trono (Addgene plasmid #12259). Human myoblasts were infected by lentivirus in growth medium. Single clone was isolated, expanded, and genotyped by PCR and Sanger sequencing. Specifically, for genotyping, PCR products were gel-purified and cloned into the TA vector (Thermo Fisher Scientific, K460001) before sequencing. MymX/MymK dKO cell line was generated from MymX^{KO} clone G6 with MymK gRNAs.

Retroviral vector preparations and expression
Retroviral vector pMXs-Puro (Cell Biolabs, #RTV-012) was used for complementary DNA (cDNA) cloning and to achieve gene overexpression. The identities of the DNA inserts in the plasmids were verified by Sanger sequencing. The MyoD-pCLBabe plasmid (59) was a gift from S. Tapscott (Addgene plasmid #20917). The

pBabe-X-SF1-myomaker plasmid was a gift from E. Olson (*60*). For all rescue experiments, gRNA-insensitive DNA cassettes were used. Two micrograms of retroviral plasmid DNA was transfected into packaging human embryonic kidney (HEK) 293 cells using FuGENE 6 (Promega, #E2692). Two days after transfection, virus medium was filtered and used to infect cells. One day after infection, the cells were switched to growth medium. For fusion rescue experiments, the cells were then switched to myoblast differentiation medium (2% horse serum in DMEM with 1% penicillin-streptomycin).

Differentiation index and fusion index measurements
Human myoblasts can be fully differentiated after 3-day induction, after which the myotubes will detach from culture dish. Therefore, unless otherwise required for a longer time, differentiation was induced for 3 days or shorter time. Differentiation index was measured as the percentage of the nuclei number in MF20+ cells relative to the total nuclei number. Fusion index was measured as the nuclei number in myotubes (three or more nuclei) as a percentage of the total number of nuclei.

GFP and Cherry labeling and cell mixing assays
Lentiviruses expressing green fluorescent protein (GFP) and retroviruses expressing Cherry were packaged from pLOVE-GFP and pMXs-Cherry (Cell Biolabs, #RTV-012) plasmids, respectively. The pLOVE-GFP plasmid (*61*) was a gift from M. Ramalho-Santos (Addgene plasmid #15949). Twelve hours before transfection, HEK293 cells were seeded in a 10-cm dish at a density of 2×10^6. Cells were infected for 2 days before use for experiments. Human myoblasts were infected by either retroviral Cherry or lentiviral GFP. The labeled cells were mixed at a 1:1 ratio and cultured in growth medium for 1 day before switching to differentiation medium for another 3 days.

Total RNA extraction, cDNA synthesis, and real-time PCR
Total RNA was extracted from cells using TRIzol Reagent (Thermo Fisher Scientific) according to the manufacturer's instructions. The quality and concentration of total RNA were assessed with a spectrophotometer (NanoDrop One, Thermo Fisher Scientific) at 260 and 280 nm. Ratios of absorption (260/280 nm) of all samples were between 1.8 and 2.0. cDNA was synthesized from 2 µg of total RNA by reverse transcription using random primers with M-MLV (Moloney Murine Leukemia Virus) reverse transcriptase (Invitrogen). Real-time PCR was performed using the QuantStudio 3 Real-Time PCR System (Thermo Fisher Scientific) with SYBR Green Master Mix (Roche) and gene-specific primers. The $2^{\Delta\Delta Ct}$ method was used to analyze gene expression after normalization with 18*S* ribosomal RNA (rRNA). Primer sequences are listed in table S1.

Membrane fractionations
Membrane fractionation was performed with the Mem-PERTM Plus Membrane Protein Extraction Kit (Thermo Fisher Scientific, 89842). Briefly, human myoblasts were suspended in phosphate-buffered saline (PBS) by scraping off the surface of the plate with a cell scraper. After centrifugation, the cell pellets were washed twice and permeabilized with constant mixing for 10 min at 4°C. The cytosol fraction (supernatant) was collected after 15-min centrifugation at 16,000*g* at 4°C. The total membrane protein fraction (pellets) was resuspended and solubilized at 4°C for 30 min with constant mixing. The membrane fraction was collected as the supernatant after 16,000*g* centrifu-

gation for 15 min at 4°C. The protein samples were mixed with 4× Laemmli sample buffer and analyzed by Western blot analysis.

Western blotting analyses
Cells were lysed in radioimmunoprecipitation assay buffer (Sigma-Aldrich, R0278) supplemented with complete protease inhibitor (Sigma-Aldrich) for 15 min. Lysates were then centrifuged at 16,000*g* for 15 min at 4°C. Protein supernatant was collected and mixed with 4× Laemmli sample buffer (Bio-Rad, #161-0747). A total of 20 to 40 µg of protein was loaded and separated by SDS–polyacrylamide gel electrophoresis. The proteins were transferred to a polyvinylidene fluoride membrane, blocked in 5% fat-free milk for 1 hour at room temperature, and then incubated with primary antibodies diluted in 5% milk overnight at 4°C. After washing in TBST (Tris buffered saline with Tween 20), the membrane was incubated with secondary antibody in blocking buffer for 1 hour at room temperature. Immunodetection was performed using Western Blotting Luminol Reagent (Thermo Fisher Scientific, 34075).

MyoD^ER expression and chemical treatments
The lentiviral pLv-CMV-MyoD-ER(T) vector (*47*) was a gift from J. Chamberlain (Addgene plasmid #26809). The lentiviruses were prepared as introduced above. Human myoblasts or mouse 3T3-HA fibroblasts were cultured in the growth medium for 18 hours and then infected by lentivirus for MyoD^ER expression. Transcriptional activity of MyoD^ER was activated by treating with 2 µM 4OH-TMX for 4 hours for mRNA measurement and 1 day for protein level measurements. CHX was added 1 hour before the application of 4OH-TMX. Total RNA was extracted from the cells for cDNA synthesis and qPCR measurements.

CRISPRi and CRISPRa assays
The lentiMPH v2 plasmid (*62*) was a gift from F. Zhang (Addgene plasmid #89308), and lentiSAM v2 was a gift from A. Karpf (Addgene plasmid #92062). The lentiSAM v2 plasmid was used for gRNA cloning after the removal of VP64 for CRISPRi experiments. Lentivirus was packaged as introduced above. The protospacer sequences for gRNAs that target the control and E-box motif regions of human MymX and MymK promoters were as follows: control for MymX, AGCCCCACTGGATTCAGCAC; MymX, AACAGCTGTGTTCT-GGCACC; control for MymK, GCAGGAGAATCTCTTGAACC; MymK, TCACGTGGCATGTCAGCTGT.

Immunostaining and microscopy
Cells were fixed in 4% paraformaldehyde/PBS for 10 min at room temperature, permeabilized with 0.2% Triton X-100 in PBS, and blocked with 3% bovine serum albumin/PBS for 1 hour at room temperature. Cells were incubated with primary antibody overnight at 4°C, followed by incubation with Alexa Fluor–conjugated secondary antibodies. Nucleus was counterstained with Hoechst 33342. The staining was visualized on the BioTek Lionheart FX Automated Microscope. Fluorescence images were collected with a camera on the BioTek Microscope System or Olympus FV1200 Confocal Laser Scanning Microscope.

Quantification and statistical analysis
Quantification results for each experiment were based on at least three independent experiments. For image analysis, randomly chosen views were imaged. All analyses were conducted with Student's *t* test with a two-tailed distribution. Comparisons with $P < 0.05$ were considered significant.

SUPPLEMENTARY MATERIALS
Supplementary material for this article is available at http://advances.sciencemag.org/cgi/content/full/6/51/eabc4062/DC1

View/request a protocol for this paper from *Bio-protocol*.

REFERENCES AND NOTES

1. C. F. Bentzinger, Y. X. Wang, M. A. Rudnicki, Building muscle: Molecular regulation of myogenesis. *Cold Spring Harb. Perspect. Biol.* **4**, a008342 (2012).
2. G. Comai, S. Tajbakhsh, Molecular and cellular regulation of skeletal myogenesis. *Curr. Top. Dev. Biol.* **110**, 1–73 (2014).
3. Y. X. Wang, M. A. Rudnicki, Satellite cells, the engines of muscle repair. *Nat. Rev. Mol. Cell Biol.* **13**, 127–133 (2011).
4. A. S. Brack, T. A. Rando, Tissue-specific stem cells: Lessons from the skeletal muscle satellite cell. *Cell Stem Cell* **10**, 504–514 (2012).
5. A. R. Demonbreun, B. H. Biersmith, E. M. McNally, Membrane fusion in muscle development and repair. *Semin. Cell Dev. Biol.* **45**, 48–56 (2015).
6. J. D. Doles, B. B. Olwin, Muscle stem cells on the edge. *Curr. Opin. Genet. Dev.* **34**, 24–28 (2015).
7. J. H. Kim, P. Jin, R. Duan, E. H. Chen, Mechanisms of myoblast fusion during muscle development. *Curr. Opin. Genet. Dev.* **32**, 162–170 (2015).
8. S. M. Hindi, M. M. Tajrishi, A. Kumar, Signaling mechanisms in mammalian myoblast fusion. *Sci. Signal.* **6**, re2 (2013).
9. S. M. Abmayr, G. K. Pavlath, Myoblast fusion: Lessons from flies and mice. *Development* **139**, 641–656 (2012).
10. F. J. Conti, S. J. Monkley, M. R. Wood, D. R. Critchley, U. Müller, Talin 1 and 2 are required for myoblast fusion, sarcomere assembly and the maintenance of myotendinous junctions. *Development* **136**, 3597–3606 (2009).
11. D. P. Millay, J. R. O'Rourke, L. B. Sutherland, S. Bezprozvannaya, J. M. Shelton, R. Bassel-Duby, E. N. Olson, Myomaker is a membrane activator of myoblast fusion and muscle formation. *Nature* **499**, 301–305 (2013).
12. P. Bi, A. Ramirez-Martinez, H. Li, J. Cannavino, J. R. McAnally, J. M. Shelton, E. Sánchez-Ortiz, R. Bassel-Duby, E. N. Olson, Control of muscle formation by the fusogenic micropeptide myomixer. *Science* **356**, 323–327 (2017).
13. Q. Zhang, A. A. Vashisht, J. O'Rourke, S. Y. Corbel, R. Moran, A. Romero, L. Miraglia, J. Zhang, E. Durrant, C. Schmedt, S. C. Sampath, S. C. Sampath, The microprotein Minion controls cell fusion and muscle formation. *Nat. Commun.* **8**, 15664 (2017).
14. M. E. Quinn, Q. Goh, M. Kurosaka, D. G. Gamage, M. J. Petrany, V. Prasad, D. P. Millay, Myomerger induces fusion of non-fusogenic cells and is required for skeletal muscle development. *Nat. Commun.* **8**, 15665 (2017).
15. D. P. Millay, L. B. Sutherland, R. Bassel-Duby, E. N. Olson, Myomaker is essential for muscle regeneration. *Genes Dev.* **28**, 1641–1646 (2014).
16. P. Bi, J. R. McAnally, J. M. Shelton, E. Sánchez-Ortiz, R. Bassel-Duby, E. N. Olson, Fusogenic micropeptide Myomixer is essential for satellite cell fusion and muscle regeneration. *Proc. Natl. Acad. Sci. U.S.A.* **115**, 3864–3869 (2018).
17. M. J. Petrany, T. Song, S. Sadayappan, D. P. Millay, Myocyte-derived Myomaker expression is required for regenerative fusion but exacerbates membrane instability in dystrophic myofibers. *JCI Insight* **5**, e136095 (2020).
18. S. A. Di Gioia, S. Connors, N. Matsunami, J. Cannavino, M. F. Rose, N. M. Gilette, P. Artoni, N. L. de Macena Sobreira, W.-M. Chan, B. D. Webb, C. D. Robson, L. Cheng, C. Van Ryzin, A. Ramirez-Martinez, P. Mohassel, M. Leppert, M. B. Scholand, C. Grunseich, C. R. Ferreira, T. Hartman, I. M. Hayes, T. Morgan, D. M. Markie, M. Fagiolini, A. Swift, P. S. Chines, C. E. Speck-Martins, F. S. Collins, E. W. Jabs, C. G. Bönnemann, E. N. Olson; Moebius Syndrome Research Consortium, J. C. Carey, S. P. Robertson, I. Manoli, E. C. Engle, A defect in myoblast fusion underlies Carey-Fineman-Ziter syndrome. *Nat. Commun.* **8**, 16077 (2017).
19. C. Hedberg-Oldfors, C. Lindberg, A. Oldfors, Carey-Fineman-Ziter syndrome with mutations in the myomaker gene and muscle fiber hypertrophy. *Neurol. Genet.* **4**, e254 (2018).
20. S. Tajbakhsh, M. Buckingham, The birth of muscle progenitor cells in the mouse: Spatiotemporal considerations. *Curr. Top. Dev. Biol.* **48**, 225–268 (2000).
21. J. M. Hernandez-Hernandez, E. G. Garcia-Gonzalez, C. E. Brun, M. A. Rudnicki, The myogenic regulatory factors, determinants of muscle development, cell identity and regeneration. *Semin. Cell Dev. Biol.* **72**, 10–18 (2017).
22. P. S. Zammit, Function of the myogenic regulatory factors Myf5, MyoD, Myogenin and MRF4 in skeletal muscle, satellite cells and regenerative myogenesis. *Semin. Cell Dev. Biol.* **72**, 19–32 (2017).
23. L. Kassar-Duchossoy, B. Gayraud-Morel, D. Gomès, D. Rocancourt, M. Buckingham, V. Shinin, S. Tajbakhsh, Mrf4 determines skeletal muscle identity in Myf5:Myod double-mutant mice. *Nature* **431**, 466–471 (2004).
24. J. K. Yoon, E. N. Olson, H. H. Arnold, B. J. Wold, Different MRF4 knockout alleles differentially disrupt Myf-5 expression: Cis-regulatory interactions at the MRF4/Myf-5 locus. *Dev. Biol.* **188**, 349–362 (1997).
25. M. A. Rudnicki, T. Braun, S. Hinuma, R. Jaenisch, Inactivation of MyoD in mice leads to up-regulation of the myogenic HLH gene Myf-5 and results in apparently normal muscle development. *Cell* **71**, 383–390 (1992).
26. M. A. Rudnicki, P. N. Schnegelsberg, R. H. Stead, T. Braun, H. H. Arnold, R. Jaenisch, Myod or Myf-5 is required for the formation of skeletal-muscle. *Cell* **75**, 1351–1359 (1993).
27. M. Yamamoto, N. P. Legendre, A. A. Biswas, A. Lawton, S. Yamamoto, S. Tajbakhsh, G. Kardon, D. J. Goldhamer, Loss of MyoD and Myf5 in skeletal muscle stem cells results in altered myogenic programming and failed regeneration. *Stem Cell Rep.* **10**, 956–969 (2018).
28. P. Hasty, A. Bradley, J. H. Morris, D. G. Edmondson, J. M. Venuti, E. N. Olson, W. H. Klein, Muscle deficiency and neonatal death in mice with a targeted mutation in the myogenin gene. *Nature* **364**, 501–506 (1993).
29. Y. Nabeshima, K. Hanaoka, M. Hayasaka, E. Esumi, S. Li, I. Nonaka, Y. Nabeshima, Myogenin gene disruption results in perinatal lethality because of severe muscle defect. *Nature* **364**, 532–535 (1993).
30. J. M. Venuti, J. H. Morris, J. L. Vivian, E. N. Olson, W. H. Klein, Myogenin is required for late but not early aspects of myogenesis during mouse development. *J. Cell Biol.* **128**, 563–576 (1995).
31. A. Rawls, J. H. Morris, M. Rudnicki, T. Braun, H. H. Arnold, W. H. Klein, E. N. Olson, Myogenin's functions do not overlap with those of MyoD or Myf-5 during mouse embryogenesis. *Dev. Biol.* **172**, 37–50 (1995).
32. M. Ganassi, S. Badodi, H. P. O. Quiroga, P. S. Zammit, Y. Hinits, S. M. Hughes, Myogenin promotes myocyte fusion to balance fibre number and size. *Nat. Commun.* **9**, 4232 (2018).
33. Y. Si, H. Wen, S. Du, Genetic mutations in jamb, jamc, and myomaker revealed different roles on myoblast fusion and muscle growth. *Mar. Biotechnol. (N.Y.)* **21**, 111–123 (2019).
34. J. Shi, P. Bi, J. Pei, H. Li, N. V. Grishin, R. Bassel-Duby, E. H. Chen, E. N. Olson, Requirement of the fusogenic micropeptide myomixer for muscle formation in zebrafish. *Proc. Natl. Acad. Sci. U.S.A.* **114**, 11950–11955 (2017).
35. W. Zhang, S. Roy, Myomaker is required for the fusion of fast-twitch myocytes in the zebrafish embryo. *Dev. Biol.* **423**, 24–33 (2017).
36. K. Mamchaoui, C. Trollet, A. Bigot, E. Negroni, S. Chaouch, A. Wolff, P. K. Kandalla, S. Marie, J. D. Santo, J. L. St. Guily, F. Muntoni, J. Kim, S. Philippi, S. Spuler, N. Levy, S. C. Blumen, T. Voit, W. E. Wright, A. Aamiri, G. Butler-Browne, V. Mouly, Immortalized pathological human myoblasts: Towards a universal tool for the study of neuromuscular disorders. *Skelet. Muscle* **1**, 34 (2011).
37. Y. Cao, R. M. Kumar, B. H. Penn, C. A. Berkes, C. Kooperberg, L. A. Boyer, R. A. Young, S. J. Tapscott, Global and gene-specific analyses show distinct roles for Myod and Myog at a common set of promoters. *EMBO J.* **25**, 502–511 (2006).
38. B. Kablar, K. Krastel, C. Ying, A. Asakura, S. J. Tapscott, M. A. Rudnicki, MyoD and Myf-5 differentially regulate the development of limb versus trunk skeletal muscle. *Development* **124**, 4729–4738 (1997).
39. L. A. Sabourin, A. Girgis-Gabardo, P. Seale, A. Asakura, M. A. Rudnicki, Reduced differentiation potential of primary MyoD–/– myogenic cells derived from adult skeletal muscle. *J. Cell Biol.* **144**, 631–643 (1999).
40. S. Tajbakhsh, D. Rocancourt, M. Buckingham, Muscle progenitor cells failing to respond to positional cues adopt non-myogenic fates in myf-5 null mice. *Nature* **384**, 266–270 (1996).
41. N. Liu, B. R. Nelson, S. Bezprozvannaya, J. M. Shelton, J. A. Richardson, R. Bassel-Duby, E. N. Olson, Requirement of MEF2A, C, and D for skeletal muscle regeneration. *Proc. Natl. Acad. Sci. U.S.A.* **111**, 4109–4114 (2014).
42. J. D. Molkentin, B. L. Black, J. F. Martin, E. N. Olson, Cooperative activation of muscle gene expression by MEF2 and myogenic bHLH proteins. *Cell* **83**, 1125–1136 (1995).
43. M. Santolini, I. Sakakibara, M. Gauthier, F. Ribas-Aulinas, H. Takahashi, T. Sawasaki, V. Mouly, J.-P. Concordet, P.-A. Defossez, V. Hakim, P. Maire, MyoD reprogramming requires Six1 and Six4 homeoproteins: Genome-wide cis-regulatory module analysis. *Nucleic Acids Res.* **44**, 8621–8640 (2016).
44. V. D. Soleimani, H. Yin, A. Jahani-Asl, H. Ming, C. E. M. Kockx, W. F. J. van Ijcken, F. Grosveld, M. A. Rudnicki, Snail regulates MyoD binding-site occupancy to direct enhancer switching and differentiation-specific transcription in myogenesis. *Mol. Cell* **47**, 457–468 (2012).
45. Y. Cao, Z. Yao, D. Sarkar, M. Lawrence, G. J. Sanchez, M. H. Parker, K. L. MacQuarrie, J. Davison, M. T. Morgan, W. L. Ruzzo, R. C. Gentleman, S. J. Tapscott, Genome-wide MyoD binding in skeletal muscle cells: A potential for broad cellular reprogramming. *Dev. Cell* **18**, 662–674 (2010).
46. A. Dall'Agnese, L. Caputo, C. Nicoletti, J. di Iulio, A. Schmitt, S. Gatto, Y. Diao, Z. Ye, M. Forcato, R. Perera, S. Bicciato, A. Telenti, B. Ren, P. L. Puri, Transcription factor-directed re-wiring of chromatin architecture for somatic cell nuclear reprogramming toward trans-differentiation. *Mol. Cell* **76**, 453, 472.e8 (2019).
47. E. Kimura, J. J. Han, S. Li, B. Fall, J. Ra, M. Haraguchi, S. J. Tapscott, J. S. Chamberlain, Cell-lineage regulated myogenesis for dystrophin replacement: A novel therapeutic approach for treatment of muscular dystrophy. *Hum. Mol. Genet.* **17**, 2507–2517 (2008).

48. C. E. Grant, T. L. Bailey, W. S. Noble, FIMO: Scanning for occurrences of a given motif. *Bioinformatics* **27**, 1017–1018 (2011).

49. F. Yue, Y. Cheng, A. Breschi, J. Vierstra, W. Wu, T. Ryba, R. Sandstrom, Z. Ma, C. Davis, B. D. Pope, Y. Shen, D. D. Pervouchine, S. Djebali, R. E. Thurman, R. Kaul, E. Rynes, A. Kirilusha, G. K. Marinov, B. A. Williams, D. Trout, H. Amrhein, K. Fisher-Aylor, I. Antoshechkin, G. De Salvo, L.-H. See, M. Fastuca, J. Drenkow, C. Zaleski, A. Dobin, P. Prieto, J. Lagarde, G. Bussotti, A. Tanzer, O. Denas, K. Li, M. A. Bender, M. Zhang, R. Byron, M. T. Groudine, D. M. Cleary, L. Pham, Z. Ye, S. Kuan, L. Edsall, Y.-C. Wu, M. D. Rasmussen, M. S. Bansal, M. Kellis, C. A. Keller, C. S. Morrissey, T. Mishra, D. Jain, N. Dogan, R. S. Harris, P. Cayting, T. Kawli, A. P. Boyle, G. Euskirchen, A. Kundaje, S. Lin, Y. Lin, C. Jansen, V. S. Malladi, M. S. Cline, D. T. Erickson, V. M. Kirkup, K. Learned, C. A. Sloan, K. R. Rosenbloom, B. L. de Sousa, K. Beal, M. Pignatelli, P. Flicek, J. Lian, T. Kahveci, D. Lee, W. J. Kent, M. R. Santos, J. Herrero, C. Notredame, A. Johnson, S. Vong, K. Lee, D. Bates, F. Neri, M. Diegel, T. Canfield, P. J. Sabo, M. S. Wilken, T. A. Reh, E. Giste, A. Shafer, T. Kutyavin, E. Haugen, D. Dunn, A. P. Reynolds, S. Neph, R. Humbert, R. S. Hansen, M. De Bruijn, L. Selleri, A. Rudensky, S. Josefowicz, R. Samstein, E. E. Eichler, S. H. Orkin, D. Levasseur, T. Papayannopoulou, K.-H. Chang, A. Skoultchi, S. Gosh, C. Disteche, P. Treuting, Y. Wang, M. J. Weiss, G. A. Blobel, X. Cao, S. Zhong, T. Wang, P. J. Good, R. F. Lowdon, L. B. Adams, X.-Q. Zhou, M. J. Pazin, E. A. Feingold, B. Wold, J. Taylor, A. Mortazavi, S. M. Weissman, J. A. Stamatoyannopoulos, M. P. Snyder, R. Guigo, T. R. Gingeras, D. M. Gilbert, R. C. Hardison, M. A. Beer, B. Ren; Mouse ENCODE Consortium, A comparative encyclopedia of DNA elements in the mouse genome. *Nature* **515**, 355–364 (2014).

50. S. Konermann, M. D. Brigham, A. E. Trevino, J. Joung, O. O. Abudayyeh, C. Barcena, P. D. Hsu, N. Habib, J. S. Gootenberg, H. Nishimasu, O. Nureki, F. Zhang, Genome-scale transcriptional activation by an engineered CRISPR-Cas9 complex. *Nature* **517**, 583–588 (2015).

51. M. H. Larson, L. A. Gilbert, X. Wang, W. A. Lim, J. S. Weissman, L. S. Qi, CRISPR interference (CRISPRi) for sequence-specific control of gene expression. *Nat. Protoc.* **8**, 2180–2196 (2013).

52. L. S. Qi, M. H. Larson, L. A. Gilbert, J. A. Doudna, J. S. Weissman, A. P. Arkin, W. A. Lim, Repurposing CRISPR as an RNA-guided platform for sequence-specific control of gene expression. *Cell* **152**, 1173–1183 (2013).

53. S. J. Tapscott, The circuitry of a master switch: Myod and the regulation of skeletal muscle gene transcription. *Development* **132**, 2685–2695 (2005).

54. M. M. Schuierer, C. J. Mann, H. Bildsoe, C. Huxley, S. M. Hughes, Analyses of the differentiation potential of satellite cells from myoD−/−, mdx, and PMP22 C22 mice. *BMC Musculoskelet. Disord.* **6**, 15 (2005).

55. Z. Yablonka-Reuveni, M. A. Rudnicki, A. J. Rivera, A. Primig, J. E. Anderson, P. Natanson, The transition from proliferation to differentiation is delayed in satellite cells from mice lacking MyoD. *Dev. Biol.* **210**, 440–455 (1999).

56. D. D. Cornelison, B. B. Olwin, M. A. Rudnicki, B. J. Wold, MyoD(−/−) satellite cells in single-fiber culture are differentiation defective and MRF4 deficient. *Dev. Biol.* **224**, 122–137 (2000).

57. M. L. Conerly, Z. Z. Yao, J. W. Zhong, M. Groudine, S. J. Tapscott, Distinct activities of Myf5 and MyoD indicate separate roles in skeletal muscle lineage specification and differentiation. *Dev. Cell* **36**, 375–385 (2016).

58. N. E. Sanjana, O. Shalem, F. Zhang, Improved vectors and genome-wide libraries for CRISPR screening. *Nat. Methods* **11**, 783–784 (2014).

59. Z. Yang, K. L. M. Quarrie, E. Analau, A. E. Tyler, F. J. Dilworth, Y. Cao, S. J. Diede, S. J. Tapscott, MyoD and E-protein heterodimers switch rhabdomyosarcoma cells from an arrested myoblast phase to a differentiated state. *Genes Dev.* **23**, 694–707 (2009).

60. D. P. Millay, D. G. Gamage, M. E. Quinn, Y.-L. Min, Y. Mitani, R. Bassel-Duby, E. N. Olson, Structure-function analysis of myomaker domains required for myoblast fusion. *Proc. Natl. Acad. Sci. U.S.A.* **113**, 2116–2121 (2016).

61. R. Blelloch, M. Venere, J. Yen, M. Ramalho-Santos, Generation of induced pluripotent stem cells in the absence of drug selection. *Cell Stem Cell* **1**, 245–247 (2007).

62. J. Joung, S. Konermann, J. S. Gootenberg, O. O. Abudayyeh, R. J. Platt, M. D. Brigham, N. E. Sanjana, F. Zhang, Genome-scale CRISPR-Cas9 knockout and transcriptional activation screening. *Nat. Protoc.* **12**, 828–863 (2017).

Citation: H. Zhang, J. Wen, A. Bigot, J. Chen, R. Shang, V. Mouly, P. Bi, Human myotube formation is determined by MyoD–Myomixer/Myomaker axis. *Sci. Adv.* **6**, eabc4062 (2020).

Science Advances

Human myotube formation is determined by MyoD–Myomixer/Myomaker axis

Haifeng Zhang, Junfei Wen, Anne Bigot, Jiacheng Chen, Renjie Shang, Vincent Mouly and Pengpeng Bi

ARTICLE TOOLS	http://advances.sciencemag.org/content/6/51/eabc4062
SUPPLEMENTARY MATERIALS	http://advances.sciencemag.org/content/suppl/2020/12/14/6.51.eabc4062.DC1
REFERENCES	This article cites 62 articles, 17 of which you can access for free http://advances.sciencemag.org/content/6/51/eabc4062#BIBL
PERMISSIONS	http://www.sciencemag.org/help/reprints-and-permissions

Use of this article is subject to the Terms of Service